

Efficient Online Inference of Vision Transformers by Training-Free Tokenization

Leonidas Gee^{1*} Wing Yan Li² Viktoriia Sharmanska¹ Novi Quadrianto^{1,3,4}

¹Predictive Analytics Lab, University of Sussex, UK ²University of Surrey, UK

³Basque Center for Applied Mathematics, Spain ⁴Monash University, Indonesia

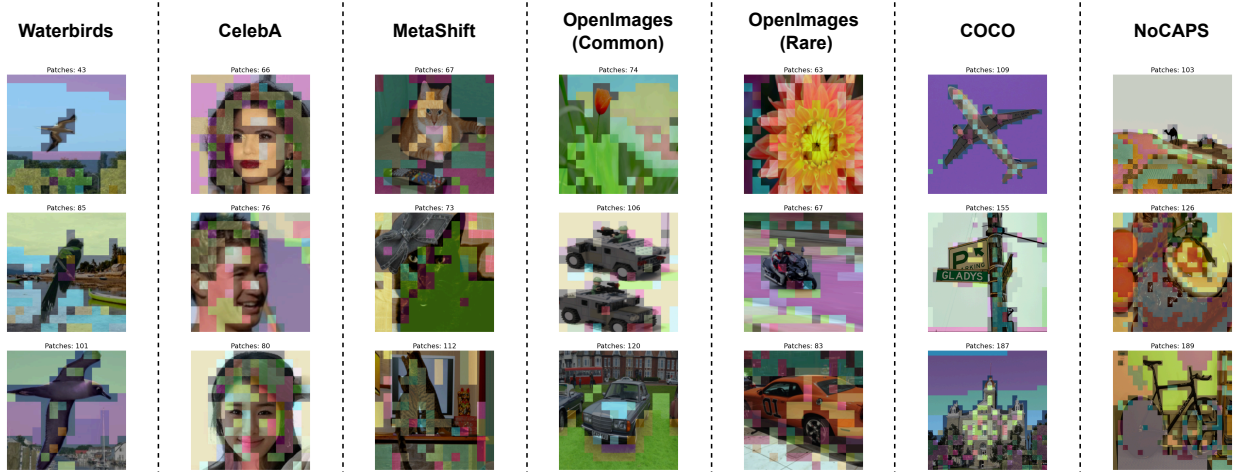


Figure 1. Visualization of patch matching by our visual word tokenizer ($\mathcal{T}_{inter}^{100}$ model). Patches that are matched with one another are indicated by identical colors. Higher patch matching is exhibited by the background rather than foreground object across the datasets. The patch matching of $\mathcal{T}_{inter}^{100}$ serves as a rudimentary form of image segmentation by grouping similar non-adjacent visual concepts.

Abstract

The cost of deploying vision transformers increasingly represents a barrier to wider industrial adoption. Existing compression requires additional end-to-end fine-tuning or incurs a significant drawback to runtime, thus making them ill-suited for online inference. We introduce the **Visual Word Tokenizer** (VWT), a training-free method for reducing energy costs while retaining performance and runtime. The VWT groups patches (visual subwords) that are frequently used into visual words while infrequent ones remain intact. To do so, intra-image or inter-image statistics are leveraged to identify similar visual concepts for compression. Experimentally, we demonstrate a reduction in wattage of up to 19% with only a 20% increase in runtime at most. Comparative approaches of 8-bit quantization and token merging achieve a lower or similar energy efficiency but exact a higher toll on runtime (up to $2\times$ or more). Our results indicate that VWTs are well-suited for efficient online inference with a marginal compromise on performance.

1. Introduction

In recent years, deep learning has seen continuous integration into a variety of systems worldwide. From coding to gaming, neural networks are increasingly deployed in online scenarios, where asynchronous requests are processed in real-time. However, due to the size and complexity of modern architectures, such models are costly to run in practice. Various methods have been proposed to improve model efficiency such as Knowledge Distillation [22], Pruning [21, 38], and Quantization [11]. However, many of these methods either require end-to-end fine-tuning to recover performance or significantly reduce runtime.

* Corresponding author: jg717@sussex.ac.uk.

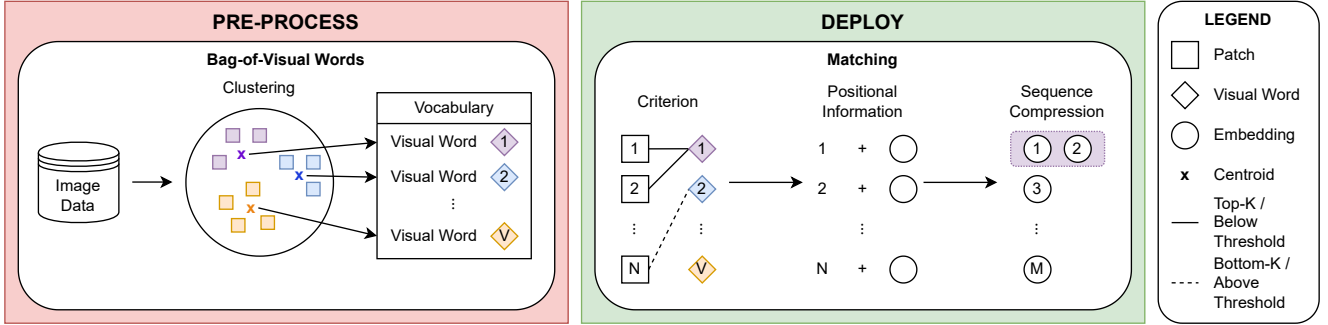


Figure 2. Overview of the Visual Word Tokenizer. (a) An intra-image approach. In the forward pass, the pixel variance of the patches is computed with bottom-k values being masked. Grouped tokens are dropped after positional information is added. Note that $V = 1$ as only a single pixel variance feature is used. (b) An inter-image approach. A Bag-of-Visual Words is formed by clustering patches in the image space. In the forward pass, the minimum pairwise cosine distance between the patches and visual words is computed with values above the threshold being masked. Grouped tokens are averaged after positional information is added.

In the field of Natural Language Processing (NLP), there is a growing trend towards improving efficiency via tokenization [9, 18, 19, 40, 61]. Newer large language models (LLMs) [14, 53] exhibit a noticeably larger vocabulary than their earlier counterparts [12, 42], thereby producing shorter sequences across various distributions. For computer vision, increasing interest is placed on reducing the cost of deploying the vision transformer (ViT) [13]. As image encoders in larger vision-language systems, ViTs are used to process images as fixed sets of tokens. Similar to downsampling in convolutional neural networks, most research [4, 5, 24, 25, 30, 37, 45] has focused on merging and/or pruning tokens in the intermediate layers to reduce computational overhead. Given the analogous architecture of the transformer across image and text modalities, our work looks instead at the idea of tokenization for efficiency by splitting an image into variable sets of tokens.

To introduce variability, we draw inspiration from subword tokenization algorithms used in NLP which follow the principle that common words should remain intact while infrequent words are broken down into meaningful subword units. Instead of a top-down approach – splitting words into subwords, our work for image data takes a bottom-up approach by grouping visual subwords (image patches) into visual words. We also twist the underlying principle: frequently used image patches should be grouped as they are more likely to describe common features or backgrounds while infrequent ones remain intact as they might carry task-relevant information. We propose two procedures to capture this principle. The first is an *intra*-image approach where patches with the lowest pixel variance within each image are grouped as they are more likely to represent uniform areas (e.g. backgrounds). The second is an *inter*-image approach, where basic features across multiple images such as colors or edges are discovered as visual words. Image patches are then grouped based on the similarity of these basic characteristics. Crucially, image patches that have distinct characteristics (i.e. high dissimilarity with any visual word) remain intact and form visual subwords. The code for our paper is publicly available¹.

2. Related Work

Efficient ViTs. Most works for improving the efficiency of ViTs have focused on reducing tokens in the intermediate layers by leveraging importance scores. In [4, 25, 30, 60], redundancy is addressed by fusing tokens. Both [45] and [50] opt to prune such tokens instead. Recent efforts [6–8, 24] attempt to combine the benefits of merging and pruning. In [54], an additional metric termed the energy score is used to better identify redundancy. Uniquely, [16] use inverse transform sampling to select important tokens. Most relevant to our work are [37] and [5]. The former assigns tokens to centroids via clustering, while the latter progressively merges tokens in a training-free manner.

Specialized Tokenizers. Our method also takes inspiration from works in NLP for efficient inference. Increasingly, the tokenizer’s vocabulary is specialized to reduce the token length of the given distribution. In [18], domain adaptation of the tokenizer by *Fast Vocabulary Transfer* (FVT) ensures fewer subword or character tokens are produced. [19] followed up by introducing n-grams for tokenization beyond the word-level boundary. Vocabulary specialization coupled with FVT has also been shown to accelerate code generation for modern LLMs [9]. Meanwhile, [61] analyzed the effectiveness of various

¹<https://github.com/wearepal/visual-word-tokenizer>

vocabulary adaptation techniques for efficient cross-lingual inference. Recently, [40] leveraged hypernetworks for zero-shot tokenizer transfer of newly domain-adapted vocabularies.

Vector Quantization. The idea of discretizing continuous distributions has been explored in many works, most recently for image generation. [62] leveraged clustering for learning a codebook that maps keypoint descriptors to discrete visual words. In [3, 58], discretization is applied as part of the modeling for ViTs. [55] learned discrete image representations by introducing the *Vector Quantised-Variational Autoencoder* (VQ-VAE) approach. [15] and [65] further improved upon the VQ-VAE by combining the expressiveness of transformers with an adversarial framework. Increasingly, vision-language models paired with codebooks conduct image synthesis autoregressively [35, 36, 44, 49, 51, 52, 66]. Lastly, [63] tackled disentangled representation learning and scene decomposition by tokenizing images into visual concepts.

3. Visual Word Tokenizer

In ViTs, tokenization is a process that splits an image into patches (tokens) which are then projected into a series of embeddings. The number of patches is typically fixed (e.g. 197) based on the choice of architecture and hyperparameters. We seek to split the image into variable length inputs instead (i.e. certain images will use 80 tokens, while others a 100). This variability is induced by conventional text tokenizers [17, 26, 48, 59] for model efficiency. We propose to achieve this via visual words that group patches (visual subwords) based on some commonality in the image space. These visual words capture frequently used patches while retaining infrequent ones as is. A simple yet effective grouping can be done using either a criterion that looks at statistics of only one image (an intra-image approach) or across many images (an inter-image approach). Figure 2 summarizes the **Visual Word Tokenizer** (VWT).

3.1. An intra-image approach

The pixel variance of the image patches is the simplest criterion that can be used for grouping. In Figure 2, this approach only utilizes the DEPLOY step by grouping the top-k patches with the lowest pixel variance while leaving the rest separate. To compress the grouped tokens, we opt to drop them as they tend to exhibit excessive homogeneity. We do not include the [CLS] token for dropping. This approach is inspired by [39] which aimed to reduce the training cost of OWLv2, an open-vocabulary object detector. Dropping patches with the lowest pixel variance removes padding areas and uniform backgrounds from the input mosaics of raw images, thus increasing training efficiency.

3.2. An inter-image approach

Inspired by text tokenizers and codebooks for image generation, we propose a variable length tokenizer that statistically discovers visual words across many images. The tokenizer consists of two steps: PRE-PROCESS and DEPLOY

PRE-PROCESS. The Bag-of-Visual Words (BoVW) is a popular method for modeling images via discrete representations. In [62], k-means clustering is applied to keypoint descriptors from SIFT [34] to learn a fixed set of centroids. These centroids represent the vocabulary to which multiple descriptors are mapped in a process termed *Vector Quantization* (VQ). In our method, we adopt a variation of this framework by building the BoVW using patches from the image space. Our design choice is motivated by two main factors. First, we find keypoint descriptors to be costly for inference. In each forward pass, computing keypoints for each image would significantly increase runtime. Second, in our early experimentation, we observed that patches in the embedding space have little similarity to one another. Such issues were also described by [5], thus leading to their use of attention scores instead. Further justification for leveraging the image space is provided in Appendix B.1.

Given a dataset, we first patchify the images using the same patch size as the image encoder (e.g. 16 for ViT-B/16). We then cluster the patches via k-means to form the BoVW of a given vocabulary size, where each centroid represents a visual word. Patchification is done via basic tensor operations and not the pre-trained convolutional layer of the ViT to avoid projection into embeddings. We also execute this process in batches using the MiniBatchKMeans² algorithm due to memory constraints. Note that MiniBatchKMeans uses the Euclidean distance by design. Since clustering is done in the image space, the BoVW may be reused by other ViTs with the same patch size regardless of model type.

DEPLOY. Once the BoVW is formed, we now turn toward the process of sequence compression. One way of leveraging the BoVW would be to merge similar patches in the image space before projecting them into embeddings. However, such a naive

²from `sklearn.cluster import MiniBatchKMeans`

Dataset	Model	Base	$\mathcal{T}_{intra}^{0.5}$	$\mathcal{T}_{inter}^{100}$		$\mathcal{T}_{inter}^{1000}$		$\mathcal{T}_{inter}^{10000}$	
				In-Domain	ImageNet	In-Domain	ImageNet	In-Domain	ImageNet
Waterbirds	CLIP	197	99	125	124	144	144	165	169
CelebA				89	88	130	119	163	155
MetaShift				112	109	136	135	162	164
OpenImages (Com.)				-	114	-	136	-	162
OpenImages (Rare)				-	110	-	133	-	160
COCO	BLIP	577	289	267	264	317	312	408	405
NoCaps				-	257	-	307	-	403

Table 1. Token length per sample (including [CLS]). \mathcal{T}_{inter}^v of varying pre-processing data and vocabulary sizes are shown. Unlike text tokenizers, domain specialization (i.e. In-Domain) does not result in greater compression. Smaller vocabularies produce shorter sequences whereas larger vocabularies result in patches being increasingly matched to separate visual words.

Dataset	Model	Base	Q_8	<i>ToME</i>	$\mathcal{T}_{intra}^{0.5}$	$\mathcal{T}_{inter}^{1000}$
Waterbirds	CLIP	123.99 ± 3.07	73.89 ± 0.23	91.64 ± 0.23	110.93 ± 0.33	107.93 ± 0.21
CelebA		126.53 ± 0.75	74.47 ± 0.18	93.07 ± 0.13	114.37 ± 0.85	102.12 ± 0.20
MetaShift		123.30 ± 0.60	74.02 ± 0.43	90.96 ± 0.33	113.84 ± 2.40	105.78 ± 0.15
OpenImages (Com.)		135.05	74.80	94.63	114.62	112.67
OpenImages (Rare)		135.66	75.27	94.04	115.78	110.75
COCO	BLIP	191.74	81.68	147.23	169.77	156.25
NoCaps		185.12	81.89	149.26	175.06	155.11

(a) Wattage (watt) ↓

Dataset	Model	Base	Q_8	<i>ToME</i>	$\mathcal{T}_{intra}^{0.5}$	$\mathcal{T}_{inter}^{1000}$
Waterbirds	CLIP	8.48 ± 0.11	88.55 ± 0.10	17.04 ± 0.06	5.84 ± 0.03	9.73 ± 0.03
CelebA		8.33 ± 0.01	89.41 ± 3.30	17.25 ± 0.13	5.86 ± 0.05	9.54 ± 0.03
MetaShift		8.21 ± 0.09	89.48 ± 0.28	17.23 ± 0.34	6.01 ± 0.30	9.87 ± 0.05
OpenImages (Com.)		8.83	92.23	17.44	5.97	9.69
OpenImages (Rare)		8.60	86.00	17.04	6.19	10.02
COCO	BLIP	12.45	57.11	15.06	8.10	9.10
NoCaps		12.44	57.61	15.08	8.04	9.28

(b) Runtime (millisecond) ↓

Table 2. Wattage and runtime per sample. Compared to *Base*, VWTs reduce wattages by up to 19% with $\mathcal{T}_{inter}^{1000}$. Although Q_8 and *ToME* display lower wattages than VWTs, they induce significantly longer runtimes, especially the former. $\mathcal{T}_{intra}^{0.5}$ is consistently faster than *Base*, while $\mathcal{T}_{inter}^{1000}$ may increase runtimes by up to 20% at most (except on COCO and NoCaps).

approach will significantly degrade performance as doing so necessitates the initialization of a new linear layer for projection. To avoid this, we begin by patchifying and computing the pairwise cosine distance between the patches and BoVW. For each patch, we retain only the minimum distance. Unlike text, we are unable to obtain exact matches with images. As such, distances higher than a given threshold are masked out to ensure dissimilar patches are not merged. This allows us to ensure that infrequently used image patches remain intact. At this point, we have determined the groupings of similar patches via their connections to the same visual words. We then apply the pre-trained convolutional layer of the ViT on the original image to patchify and project it into a series of embeddings. Before merging, we ensure that positional information is added to the embeddings as we found it to work better than adding them later. Lastly, we average the embeddings element-wise based on the earlier defined groupings. We do not include the [CLS] token for merging.

For the inter-image approach, if batching instead of online inference is desired, the uniform requirement of tensors becomes a challenge. To maintain parallelism, any reduction has to be equal across samples. Due to the non-uniformity of tokenization, sequences have to be sequentially compressed before padding to the same length. We opt to append additional

Model	Waterbirds		CelebA		MetaShift		OpenImages	
	Average \uparrow	Worst \uparrow	Average \uparrow	Worst \uparrow	Average \uparrow	Worst \uparrow	Common \uparrow	Rare \uparrow
<i>Base</i>	79.06 \pm 0.14	21.86 \pm 0.32	89.61 \pm 0.14	47.21 \pm 2.41	95.31 \pm 1.00	87.69 \pm 3.08	70.48	63.36
Q_8	79.94 \pm 0.20	24.25 \pm 0.09	89.73 \pm 0.13	48.19 \pm 3.24	95.23 \pm 0.74	88.21 \pm 3.87	70.48	63.19
<i>ToME</i>	79.80 \pm 0.15	27.05 \pm 0.09	89.25 \pm 0.15	28.52 \pm 4.49	94.24 \pm 0.43	87.37 \pm 3.01	65.69	60.05
$\mathcal{T}_{intra}^{0.5}$	75.56 \pm 0.06	31.00 \pm 0.47	89.27 \pm 0.12	50.93 \pm 1.16	92.94 \pm 0.35	86.15 \pm 2.66	65.52	59.73
$\mathcal{T}_{inter}^{1000}$	79.19 \pm 0.10	23.83 \pm 0.27	90.79 \pm 0.15	47.96 \pm 4.98	93.94 \pm 0.70	86.67 \pm 2.35	66.15	60.56

(a) CLIP (image classification and group robustness)

Model	COCO		NoCaps							
	Karpathy \uparrow		In-Domain \uparrow		Near-Domain \uparrow		Out-of-Domain \uparrow		Overall \uparrow	
	BLEU@4	CIDEr	CIDEr	SPICE	CIDEr	SPICE	CIDEr	SPICE	CIDEr	SPICE
<i>Base</i>	34.00	107.35	103.57	14.60	98.87	14.11	92.96	13.30	98.34	14.02
Q_8	33.85	106.87	103.86	14.53	100.07	14.18	92.72	13.49	99.12	14.10
<i>ToME</i>	30.02	94.40	97.35	14.42	90.74	13.39	84.22	12.69	90.37	13.40
$\mathcal{T}_{intra}^{0.5}$	32.80	104.37	99.86	14.20	94.21	13.73	89.52	13.12	94.07	13.68
$\mathcal{T}_{inter}^{1000}$	32.12	101.79	98.19	13.95	93.85	13.49	86.03	12.67	92.89	13.39

(b) BLIP (image captioning)

Table 3. Zero-shot image classification (CLIP), group robustness (CLIP) and captioning (BLIP). VWTs maintain average accuracy relative to *Base* while improving robustness on Waterbirds. On COCO and NoCaps, VWTs retains a higher performance than *ToME*.

[PAD] tokens until the longest length within the batch is achieved. Similar to text transformers [56], the attention scores are set to negative infinity before the softmax to nullify the influence of padding. We do not add positional information to the [PAD] tokens as extrapolating such information to non-uniform sequences will significantly worsen model efficiency.

4. Experiments

Consider a pre-trained image encoder $f \in \mathcal{F}$ with parameters $\theta \in \Theta$ that transforms inputs $x \in \mathcal{X} \subseteq \mathbb{R}^d$ to encodings $\hat{x} \in \mathcal{X} \subseteq \mathbb{R}^d$. The encodings can then be mapped to labels $y \in \mathcal{Y}$ for some given task, be it classification or generation. More specifically, the ViT first transforms inputs x to tokens t_1, \dots, t_N before further processing by the attention layers. The number of tokens N is a constant defined by $(\frac{I}{P})^2$, where I and P are the image and patch sizes, respectively. Let \mathcal{T} be the VWT associated with a vocabulary $v \in \mathcal{V}$, where v is a visual word learned from some dataset D . The tokenizer transforms the input x into tokens t_1, \dots, t_M , where $M \ll N$. In our experiments, we seek to analyze the effect of \mathcal{T} on online inference efficiency. We do so through the lens of (i) performance retention in visual recognition tasks of zero-shot classification, (ii) group robustness, and (iii) generative performance of visual captioning.

Dataset and Setting. To study the effects of tokenization on (i) performance retention in visual recognition tasks of zero-shot classification, we conduct two sets of evaluations: 1) using one dataset for large-scale evaluation and 2) using three datasets for robustness analysis detailed below. We focus on a zero-shot setting by eschewing any end-to-end fine-tuning of f . For large-scale evaluation, we use the OpenImages v6 dataset [27]. Following [23], the test split is divided into *common* and *rare* subsets that consist of 57 224 and 21 991 images, respectively. The former has 214 classes, while the latter has 200. To perform classification, we compute the cosine similarity between an image embedding and the encoded text label³.

To study performance retention and (ii) group robustness in image classification, we utilize three publicly available datasets: Waterbirds [57], CelebA [33], and MetaShift [29], that are used as benchmarks in robustness and fairness research [32, 47, 64]. To perform (zero-shot) classification, we compute the cosine similarity between an image embedding and the following encoded text labels³ for Waterbirds, CelebA, and MetaShift, respectively: {'landbird', 'waterbird'}, {'non-blond', 'blond'}, {'dog', 'cat'}. The same data splits and spurious attributes as [32] and [64] are used for the former two

³The prefix "a photo of a " is also added to encode each text label.

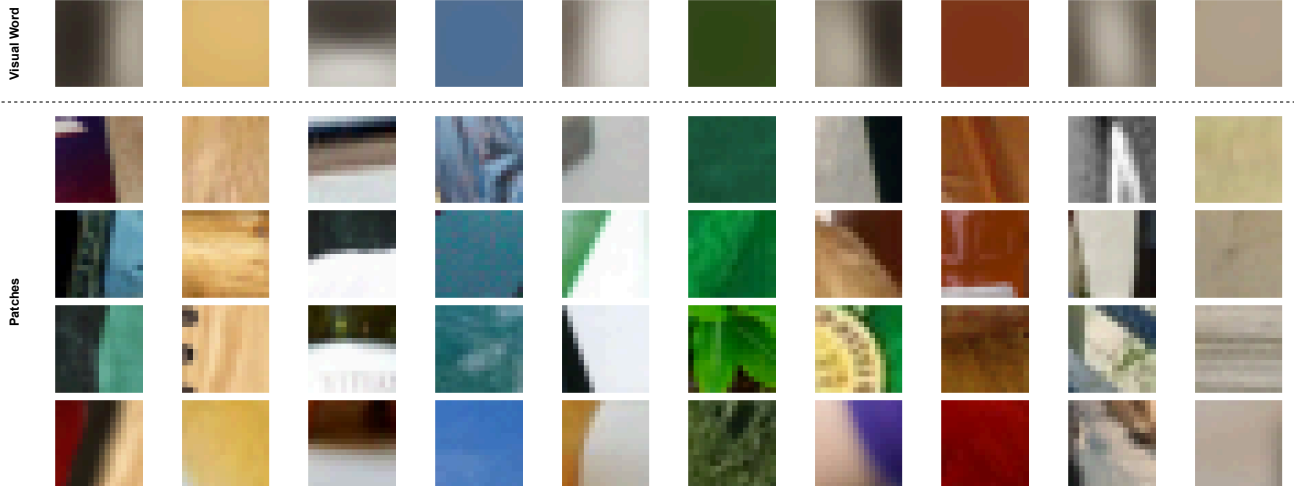


Figure 3. Visualization of the vocabulary of $\mathcal{T}_{inter}^{100}$. Patches from ImageNet-1K are matched to the closest visual word using the Euclidean distance. Visual words are shown to depict basic features such as colors or edges. As centroids, each visual word is an average representation of patches that belong to the matched cluster.

and latter datasets, respectively. Specifically, the following spurious attributes are studied: habitation {'water', 'land'} for Waterbirds, gender {'female', 'male'} for CelebA, and context {'indoor', 'outdoor'} for MetaShift. Further details on the subgroups are provided in Appendix A.1. We also compute the variance by shuffling samples among the data splits while maintaining subgroup proportions. We leverage attribute annotations not only for analyzing average and robust performance but also for the fairness of tokenization in Appendix B.4.

To analyze the effect of \mathcal{T} on (iii) generative task of image captioning, we utilize the Karpathy test split of COCO dataset [31] and a validation set of NoCaps dataset [1] following the setting in previous work [28].

Finally, to study inference efficiency, we utilize all datasets for the downstream visual tasks (i)-(iii) described above. We focus on the online setting where batch size is 1.

Baselines. For image classification, we load the pre-trained CLIP [43] model from HuggingFace⁴. The prefix "a photo of a " is also added to each text category. An image size of 224×224 is used with bilinear interpolation for CLIP. For image captioning, we load the pre-trained BLIP [28] model from HuggingFace⁵. To perform zero-shot captioning, we use a beam size of 3 along with maximum and minimum lengths of 20 and 5, respectively. Unlike [28], we do not include the prefix "a picture of " as we found it to work better. An image size of 384×384 is used with bicubic interpolation. Both CLIP and BLIP utilize the ViT-B/16 image encoder unless stated otherwise.

Aside from the pre-trained model which we denote as *Base*, we also consider 8-bit quantization [11] and token merging [5] as additional baselines. We denote the former as *Q₈* and the latter as *ToME*. Following [5], we utilize a reduction per layer for *ToME* of 13 with CLIP and 23 with BLIP due to their respective input image sizes. For the VWTs, we set the top-k of the intra-image approach to 50% of the total number of patches which we denote as $\mathcal{T}_{intra}^{0.5}$. For the inter-image approach, we set the threshold to 0.1 unless stated otherwise and denote it as $\mathcal{T}_{inter}^{\mathcal{V}}$, where \mathcal{V} is the size of the vocabulary. Lastly, our experiments are conducted using a single NVIDIA A100 GPU.

Inference Efficiency. First we analyze the effects of VWTs on token length. We seek to understand how the choice of pre-processing data and vocabulary size affects the degree of compression. Table 1 shows the token length per sample (including [CLS]) on different datasets. Unlike $\mathcal{T}_{intra}^{0.5}$, the sequence lengths induced by $\mathcal{T}_{inter}^{\mathcal{V}}$ are not equal. First, we compare $\mathcal{T}_{inter}^{\mathcal{V}}$ pre-processed on the in-domain dataset and ImageNet-1K [10]. The in-domain dataset is represented by the training split if available. On text data, in-domain tokenizers [9, 40, 61] have been shown to produce shorter sequences by specializing the vocabulary on the given distribution. Interestingly, we observe no such effect with image data as seen by the similar lengths between In-Domain and ImageNet-1K. Only on CelebA, do we see a greater reduction with $\mathcal{T}_{inter}^{1000}$ and $\mathcal{T}_{inter}^{10000}$ pre-processed

⁴<https://huggingface.co/openai/clip-vit-base-patch16>

⁵<https://huggingface.co/Salesforce/blip-image-captioning-base>

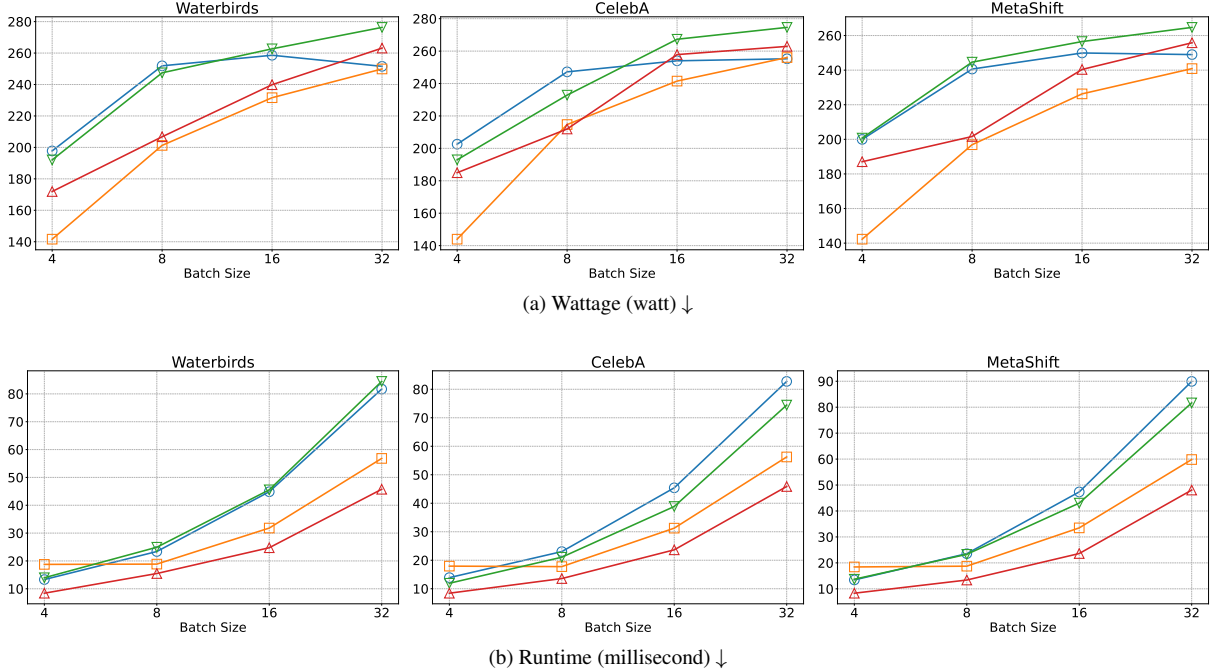


Figure 5. Wattage and runtime with varying batch sizes. $\mathcal{T}_{intra}^{0.5}$ (\triangle) and $\mathcal{T}_{inter}^{1000}$ (∇) is compared to *Base* (\circ) and *ToME* (\square). Unlike $\mathcal{T}_{inter}^{1000}$, which reaches wattage parity with *Base* at smaller batches, $\mathcal{T}_{intra}^{0.5}$ and *ToME* continue to show lower wattages up to a batch size of 16. Runtime also increases more for $\mathcal{T}_{inter}^{1000}$ as non-uniform sequences have to be sequentially merged before padding.

Visual Words. To better understand the inter-image approach, we visualize the patch matching of $\mathcal{T}_{inter}^{100}$ in Figure 1. We highlight in identical colors patches that are matched with one another. First, we find that patches representing the background are more frequently grouped than those of the foreground. On Waterbirds, the merging of background patches may explain the improved robustness in Table 3 by mitigating the spurious correlation with the background. On CelebA, $\mathcal{T}_{inter}^{100}$ tends to avoid matching the eyes or mouths of the individuals. Second, we observe that patch matching is capable of grouping similar but non-adjacent visual concepts. In certain examples of MetaShift and NoCaps, multiple cats and foods are seemingly matched together, respectively. Our analysis shows that patch matching serves as a rudimentary form of image segmentation.

In Figure 3, we visualize the vocabulary of $\mathcal{T}_{inter}^{100}$ to analyze the formation of the visual words. We show patches from ImageNet-1K (i.e. pre-processing data) that are matched to each visual word using the Euclidean distance. Since visual words are centroids, patches that are matched to the same visual word belong to the same cluster. We observe that visual words depict basic features such as colors or edges. These features are also formed as an average representation of the patches that belong to each cluster. By representing basic features, visual words serve as effective anchor points to which patches can be matched to. Analysis on the sparsity of the vocabularies in the inter-image approach can be found in Appendix B.5.

Long-form Captioning. The generated captions by BLIP [28] can be used as priors for further training of other models. As such, longer descriptive captions may be more desirable than the typical short captions associated with Internet data. In Figure 4, we visualize the long-form captions on COCO. To enable longer generations, we set the length penalty to 2.0 and double the maximum length to 40. All other generation settings are kept the same. With longer captions, the generation may degenerate into unnecessary repetitions on certain samples. Interestingly, descriptiveness and coherence improves more with $\mathcal{T}_{inter}^{100}$ than $\mathcal{T}_{intra}^{0.5}$ or $\mathcal{T}_{inter}^{1000}$. Additional long-form captions by Q_8 , *ToME*, and $\mathcal{T}_{inter}^{10000}$ are provided in Appendix C.1.

Batch Processing. Earlier we stated how VWTs works optimally for online inference. In Figure 5, we seek to better understand its effectiveness for *offline inference* where batch sizes are greater than 1. Using typical batches of $\{4, 8, 16, 32\}$, we compare $\mathcal{T}_{intra}^{0.5}$ and $\mathcal{T}_{inter}^{1000}$ to *Base* and *ToME*. First, we find that as batch size increases, lower wattages relative to *Base* are seen with $\mathcal{T}_{intra}^{0.5}$ and *ToME*, particularly at lower batch sizes. Both VWTs and *ToME* eventually reach wattage parity with *Base* at larger batches (i.e. 32), with $\mathcal{T}_{inter}^{1000}$ doing so much earlier. Second, we observe different runtime trends

between VWTs and *ToME*. As batches grow, $\mathcal{T}_{inter}^{1000}$ continues to show similar runtimes to *Base*. Meanwhile, $\mathcal{T}_{intra}^{0.5}$ and *ToME* display lower runtimes with the exception of batch size 4 for the latter. As such, during batching, the inter-image approach does not confer the same degree of efficiency improvements.

When to use the intra-image or inter-image approach? Concerning the choice between the intra-image or inter-image approach, we posit that when global information is required, dropping tokens may be more advantageous by removing unnecessary noise from the visual input. On the other hand, when the task necessitates local information (e.g. long-form captioning, object detection, etc.), merging tokens may better preserve the visual concepts. For example, the image on the first row of Figure 7 shows that $\mathcal{T}_{intra}^{0.5}$ removes the mountainous background, thus leading to the absence of "mountain" in the long-form caption of Figure 4. Potentially, combining both approaches may maximize compression while preserving information by merging the mountains and dropping the bushes in said image.

5. Conclusion

In this work, we set out to define a training-free tokenization for ViTs that lowers wattage while balancing costs to runtime and performance. In online scenarios, we have shown empirically that our intra-image and inter-image approaches are competitive with 8-bit quantization and token merging for image classification and captioning. Qualitatively, we observe how the inter-image approach groups analogous visual concepts via visual words that represent basic features. Analysis on large-scale classification further validates the viability of our method while long-form captioning shows its potential for improving descriptiveness and coherence. Lastly, the inter-image approach has limits for batch processing due to its non-parallelism. As a future work, further research can be made into combining both approaches.

Acknowledgements

This research was supported by a European Research Council (ERC) Starting Grant for the project "Bayesian Models and Algorithms for Fairness and Transparency", funded under the European Union's Horizon 2020 Framework Programme (grant agreement no. 851538). Novi Quadrianto is also supported by the Basque Government through the BERC 2022-2025 program and by the Ministry of Science and Innovation: BCAM Severo Ochoa accreditation CEX2021-001142-S / MICIN/AEI/ 10.13039/501100011033. Viktoriia Sharmanska is currently at Epic Games.

References

- [1] Harsh Agrawal, Karan Desai, Yufei Wang, Xinlei Chen, Rishabh Jain, Mark Johnson, Dhruv Batra, Devi Parikh, Stefan Lee, and Peter Anderson. Nocaps: Novel object captioning at scale. In *Proceedings of the IEEE/CVF international conference on computer vision*, pages 8948–8957, 2019. 6
- [2] Mehdi Ali, Michael Fromm, Klaudia Thellmann, Richard Rutmann, Max Lübbering, Johannes Leveling, Katrin Klug, Jan Ebert, Niclas Doll, Jasper Schulze Buschhoff, et al. Tokenizer choice for llm training: Negligible or crucial? *arXiv preprint arXiv:2310.08754*, 2023. 2
- [3] Hangbo Bao, Li Dong, Songhao Piao, and Furu Wei. Beit: Bert pre-training of image transformers. *arXiv preprint arXiv:2106.08254*, 2021. 3
- [4] Zhe Bian, Zhe Wang, Wenqiang Han, and Kangping Wang. Multi-scale and token merge: Make your vit more efficient. *arXiv preprint arXiv:2306.04897*, 2023. 2
- [5] Daniel Bolya, Cheng-Yang Fu, Xiaoliang Dai, Peizhao Zhang, Christoph Feichtenhofer, and Judy Hoffman. Token merging: Your vit but faster. *arXiv preprint arXiv:2210.09461*, 2022. 2, 3, 6
- [6] Maxim Bonnaerens and Joni Dambre. Learned thresholds token merging and pruning for vision transformers. *arXiv preprint arXiv:2307.10780*, 2023. 2
- [7] Qingqing Cao, Bhargavi Paranjape, and Hannaneh Hajishirzi. Pumer: Pruning and merging tokens for efficient vision language models. In *Proceedings of the 61st Annual Meeting of the Association for Computational Linguistics (Volume 1: Long Papers)*, pages 12890–12903, 2023.
- [8] Mengzhao Chen, Wenqi Shao, Peng Xu, Mingbao Lin, Kaipeng Zhang, Fei Chao, Rongrong Ji, Yu Qiao, and Ping Luo. Diffrate: Differentiable compression rate for efficient vision transformers. In *Proceedings of the IEEE/CVF International Conference on Computer Vision*, pages 17164–17174, 2023. 2
- [9] Gautier Dagan, Gabriele Synnaeve, and Baptiste Rozière. Getting the most out of your tokenizer for pre-training and domain adaptation. *arXiv preprint arXiv:2402.01035*, 2024. 2, 6
- [10] Jia Deng, Wei Dong, Richard Socher, Li-Jia Li, Kai Li, and Li Fei-Fei. Imagenet: A large-scale hierarchical image database. In *2009 IEEE conference on computer vision and pattern recognition*, pages 248–255. Ieee, 2009. 6

- [11] Tim Dettmers, Mike Lewis, Younes Belkada, and Luke Zettlemoyer. Gpt3. int8 (): 8-bit matrix multiplication for transformers at scale. *Advances in Neural Information Processing Systems*, 35:30318–30332, 2022. 1, 6
- [12] Jacob Devlin. Bert: Pre-training of deep bidirectional transformers for language understanding. *arXiv preprint arXiv:1810.04805*, 2018. 2
- [13] Alexey Dosovitskiy, Lucas Beyer, Alexander Kolesnikov, Dirk Weissenborn, Xiaohua Zhai, Thomas Unterthiner, Mostafa Dehghani, Matthias Minderer, Georg Heigold, Sylvain Gelly, et al. An image is worth 16x16 words: Transformers for image recognition at scale. *arXiv preprint arXiv:2010.11929*, 2020. 2
- [14] Abhimanyu Dubey, Abhinav Jauhri, Abhinav Pandey, Abhishek Kadian, Ahmad Al-Dahle, Aiesha Letman, Akhil Mathur, Alan Schelten, Amy Yang, Angela Fan, et al. The llama 3 herd of models. *arXiv preprint arXiv:2407.21783*, 2024. 2
- [15] Patrick Esser, Robin Rombach, and Bjorn Ommer. Taming transformers for high-resolution image synthesis. In *Proceedings of the IEEE/CVF conference on computer vision and pattern recognition*, pages 12873–12883, 2021. 3
- [16] Mohsen Fayyaz, Soroush Abbasi Koochpayegani, Farnoush Rezaei Jafari, Sunando Sengupta, Hamid Reza Vaezi Joze, Eric Sommerlade, Hamed Pirsivash, and Jürgen Gall. Adaptive token sampling for efficient vision transformers. In *European Conference on Computer Vision*, pages 396–414. Springer, 2022. 2
- [17] Philip Gage. A new algorithm for data compression. *The C Users Journal*, 12(2):23–38, 1994. 3
- [18] Leonidas Gee, Andrea Zugarini, Leonardo Rigutini, and Paolo Torrioni. Fast vocabulary transfer for language model compression. In *Proceedings of the 2022 Conference on Empirical Methods in Natural Language Processing: Industry Track*, pages 409–416, 2022. 2
- [19] Leonidas Gee, Leonardo Rigutini, Marco Erlandes, and Andrea Zugarini. Multi-word tokenization for sequence compression. In *Proceedings of the 2023 Conference on Empirical Methods in Natural Language Processing: Industry Track*, pages 612–621, 2023. 2
- [20] Leonidas Gee, Andrea Zugarini, and Novi Quadrianto. Are compressed language models less subgroup robust? In *Proceedings of the 2023 Conference on Empirical Methods in Natural Language Processing*, pages 15859–15868, 2023. 7
- [21] Song Han, Jeff Pool, John Tran, and William Dally. Learning both weights and connections for efficient neural network. *Advances in neural information processing systems*, 28, 2015. 1
- [22] Geoffrey Hinton, Oriol Vinyals, and Jeff Dean. Distilling the knowledge in a neural network. *arXiv preprint arXiv:1503.02531*, 2015. 1
- [23] Xinyu Huang, Yi-Jie Huang, Youcai Zhang, Weiwei Tian, Rui Feng, Yuejie Zhang, Yanchun Xie, Yaqian Li, and Lei Zhang. Open-set image tagging with multi-grained text supervision. *arXiv e-prints*, pages arXiv–2310, 2023. 5, 7
- [24] Minchul Kim, Shangqian Gao, Yen-Chang Hsu, Yilin Shen, and Hongxia Jin. Token fusion: Bridging the gap between token pruning and token merging. In *Proceedings of the IEEE/CVF Winter Conference on Applications of Computer Vision*, pages 1383–1392, 2024. 2
- [25] Zhenglun Kong, Peiyan Dong, Xiaolong Ma, Xin Meng, Wei Niu, Mengshu Sun, Xuan Shen, Geng Yuan, Bin Ren, Hao Tang, et al. Spvit: Enabling faster vision transformers via latency-aware soft token pruning. In *European conference on computer vision*, pages 620–640. Springer, 2022. 2
- [26] Taku Kudo and John Richardson. Sentencepiece: A simple and language independent subword tokenizer and detokenizer for neural text processing. *EMNLP 2018*, page 66, 2018. 3
- [27] Alina Kuznetsova, Hassan Rom, Neil Alldrin, Jasper Uijlings, Ivan Krasin, Jordi Pont-Tuset, Shahab Kamali, Stefan Popov, Matteo Mallocci, Alexander Kolesnikov, et al. The open images dataset v4: Unified image classification, object detection, and visual relationship detection at scale. *International journal of computer vision*, 128(7):1956–1981, 2020. 5
- [28] Junnan Li, Dongxu Li, Caiming Xiong, and Steven Hoi. Blip: Bootstrapping language-image pre-training for unified vision-language understanding and generation. In *International conference on machine learning*, pages 12888–12900. PMLR, 2022. 6, 7, 8
- [29] Weixin Liang and James Zou. Metashift: A dataset of datasets for evaluating contextual distribution shifts and training conflicts. In *International Conference on Learning Representations*, 2022. 5, 1
- [30] Youwei Liang, Chongjian Ge, Zhan Tong, Yibing Song, Jue Wang, and Pengtao Xie. Not all patches are what you need: Expediting vision transformers via token reorganizations. *arXiv preprint arXiv:2202.07800*, 2022. 2
- [31] Tsung-Yi Lin, Michael Maire, Serge Belongie, James Hays, Pietro Perona, Deva Ramanan, Piotr Dollár, and C Lawrence Zitnick. Microsoft coco: Common objects in context. In *Computer Vision—ECCV 2014: 13th European Conference, Zurich, Switzerland, September 6–12, 2014, Proceedings, Part V 13*, pages 740–755. Springer, 2014. 6
- [32] Evan Z Liu, Behzad Haghgoo, Annie S Chen, Aditi Raghunathan, Pang Wei Koh, Shiori Sagawa, Percy Liang, and Chelsea Finn. Just train twice: Improving group robustness without training group information. In *International Conference on Machine Learning*, pages 6781–6792. PMLR, 2021. 5
- [33] Ziwei Liu, Ping Luo, Xiaogang Wang, and Xiaoou Tang. Deep learning face attributes in the wild. In *Proceedings of the IEEE international conference on computer vision*, pages 3730–3738, 2015. 5, 1
- [34] David G Lowe. Distinctive image features from scale-invariant keypoints. *International journal of computer vision*, 60:91–110, 2004. 3

- [35] Jiasen Lu, Christopher Clark, Rowan Zellers, Roozbeh Mottaghi, and Aniruddha Kembhavi. Unified-io: A unified model for vision, language, and multi-modal tasks. *arXiv preprint arXiv:2206.08916*, 2022. 3
- [36] Jiasen Lu, Christopher Clark, Sangho Lee, Zichen Zhang, Savya Khosla, Ryan Marten, Derek Hoiem, and Aniruddha Kembhavi. Unified-io 2: Scaling autoregressive multimodal models with vision language audio and action. In *Proceedings of the IEEE/CVF Conference on Computer Vision and Pattern Recognition*, pages 26439–26455, 2024. 3
- [37] Dmitrii Marin, Jen-Hao Rick Chang, Anurag Ranjan, Anish Prabhu, Mohammad Rastegari, and Oncel Tuzel. Token pooling in vision transformers. *arXiv preprint arXiv:2110.03860*, 2021. 2
- [38] Paul Michel, Omer Levy, and Graham Neubig. Are sixteen heads really better than one? *Advances in neural information processing systems*, 32, 2019. 1
- [39] Matthias Minderer, Alexey Gritsenko, and Neil Houlsby. Scaling open-vocabulary object detection. *Advances in Neural Information Processing Systems*, 36, 2024. 3, 2
- [40] Benjamin Minixhofer, Edoardo Maria Ponti, and Ivan Vulić. Zero-shot tokenizer transfer. *arXiv preprint arXiv:2405.07883*, 2024. 2, 3, 6
- [41] Aleksandar Petrov, Emanuele La Malfa, Philip Torr, and Adel Bibi. Language model tokenizers introduce unfairness between languages. *Advances in Neural Information Processing Systems*, 36, 2024. 2
- [42] Alec Radford, Jeffrey Wu, Rewon Child, David Luan, Dario Amodei, Ilya Sutskever, et al. Language models are unsupervised multitask learners. *OpenAI blog*, 1(8):9, 2019. 2
- [43] Alec Radford, Jong Wook Kim, Chris Hallacy, Aditya Ramesh, Gabriel Goh, Sandhini Agarwal, Girish Sastry, Amanda Askell, Pamela Mishkin, Jack Clark, et al. Learning transferable visual models from natural language supervision. In *International conference on machine learning*, pages 8748–8763. PMLR, 2021. 6, 7
- [44] Aditya Ramesh, Mikhail Pavlov, Gabriel Goh, Scott Gray, Chelsea Voss, Alec Radford, Mark Chen, and Ilya Sutskever. Zero-shot text-to-image generation. In *International conference on machine learning*, pages 8821–8831. Pmlr, 2021. 3
- [45] Yongming Rao, Wenliang Zhao, Benlin Liu, Jiwen Lu, Jie Zhou, and Cho-Jui Hsieh. Dynamicvit: Efficient vision transformers with dynamic token sparsification. *Advances in neural information processing systems*, 34:13937–13949, 2021. 2
- [46] Sara Romiti, Christopher Inskip, Viktoriia Sharmanska, and Novi Quadrianto. Realpatch: A statistical matching framework for model patching with real samples. In *European Conference on Computer Vision*, pages 146–162. Springer, 2022. 7
- [47] Shiori Sagawa, Pang Wei Koh, Tatsunori B Hashimoto, and Percy Liang. Distributionally robust neural networks for group shifts: On the importance of regularization for worst-case generalization. *arXiv preprint arXiv:1911.08731*, 2019. 5, 7, 1
- [48] Rico Sennrich, Barry Haddow, and Alexandra Birch. Neural machine translation of rare words with subword units. In *Proceedings of the 54th Annual Meeting of the Association for Computational Linguistics (Volume 1: Long Papers)*, pages 1715–1725, 2016. 3
- [49] Peize Sun, Yi Jiang, Shoufa Chen, Shilong Zhang, Bingyue Peng, Ping Luo, and Zehuan Yuan. Autoregressive model beats diffusion: Llama for scalable image generation. *arXiv preprint arXiv:2406.06525*, 2024. 3
- [50] Yehui Tang, Kai Han, Yunhe Wang, Chang Xu, Jianyuan Guo, Chao Xu, and Dacheng Tao. Patch slimming for efficient vision transformers. In *Proceedings of the IEEE/CVF Conference on Computer Vision and Pattern Recognition*, pages 12165–12174, 2022. 2, 1
- [51] Chameleon Team. Chameleon: Mixed-modal early-fusion foundation models. *arXiv preprint arXiv:2405.09818*, 2024. 3
- [52] Gemini Team, Rohan Anil, Sebastian Borgeaud, Yonghui Wu, Jean-Baptiste Alayrac, Jiahui Yu, Radu Soricut, Johan Schalkwyk, Andrew M Dai, Anja Hauth, et al. Gemini: a family of highly capable multimodal models. *arXiv preprint arXiv:2312.11805*, 2023. 3
- [53] Gemma Team, Morgane Riviere, Shreya Pathak, Pier Giuseppe Sessa, Cassidy Hardin, Surya Bhupatiraju, Léonard Hussenot, Thomas Mesnard, Bobak Shahriari, Alexandre Ramé, et al. Gemma 2: Improving open language models at a practical size. *arXiv preprint arXiv:2408.00118*, 2024. 2
- [54] Hoai-Chau Tran, Duy MH Nguyen, Duy M Nguyen, Trung-Tin Nguyen, Ngan Le, Pengtao Xie, Daniel Sonntag, James Y Zou, Binh T Nguyen, and Mathias Niepert. Accelerating transformers with spectrum-preserving token merging. *arXiv preprint arXiv:2405.16148*, 2024. 2
- [55] Aaron Van Den Oord, Oriol Vinyals, et al. Neural discrete representation learning. *Advances in neural information processing systems*, 30, 2017. 3
- [56] Ashish Vaswani, Noam Shazeer, Niki Parmar, Jakob Uszkoreit, Llion Jones, Aidan N Gomez, Łukasz Kaiser, and Illia Polosukhin. Attention is all you need. *Advances in neural information processing systems*, 30, 2017. 5
- [57] Catherine Wah, Steve Branson, Peter Welinder, Pietro Perona, and Serge Belongie. The caltech-ucsd birds-200-2011 dataset. 2011. 5, 1
- [58] Bichen Wu, Chenfeng Xu, Xiaoliang Dai, Alvin Wan, Peizhao Zhang, Zhicheng Yan, Masayoshi Tomizuka, Joseph Gonzalez, Kurt Keutzer, and Peter Vajda. Visual transformers: Token-based image representation and processing for computer vision. *arXiv preprint arXiv:2006.03677*, 2020. 3
- [59] Yonghui Wu, Mike Schuster, Zhifeng Chen, Quoc V Le, Mohammad Norouzi, Wolfgang Macherey, Maxim Krikun, Yuan Cao, Qin Gao, Klaus Macherey, et al. Google’s neural machine translation system: Bridging the gap between human and machine translation. *arXiv preprint arXiv:1609.08144*, 2016. 3

- [60] Yifan Xu, Zhijie Zhang, Mengdan Zhang, Kekai Sheng, Ke Li, Weiming Dong, Liqing Zhang, Changsheng Xu, and Xing Sun. Evo-vit: Slow-fast token evolution for dynamic vision transformer. In *Proceedings of the AAAI Conference on Artificial Intelligence*, pages 2964–2972, 2022. [2](#)
- [61] Atsuki Yamaguchi, Aline Villavicencio, and Nikolaos Aletras. An empirical study on cross-lingual vocabulary adaptation for efficient generative llm inference. *arXiv preprint arXiv:2402.10712*, 2024. [2](#), [6](#)
- [62] Jun Yang, Yu-Gang Jiang, Alexander G Hauptmann, and Chong-Wah Ngo. Evaluating bag-of-visual-words representations in scene classification. In *Proceedings of the international workshop on Workshop on multimedia information retrieval*, pages 197–206, 2007. [3](#)
- [63] Tao Yang, Yuwang Wang, Yan Lu, and Nanning Zheng. Visual concepts tokenization. *Advances in Neural Information Processing Systems*, 35:31571–31582, 2022. [3](#)
- [64] Yuzhe Yang, Haoran Zhang, Dina Katabi, and Marzyeh Ghassemi. Change is hard: A closer look at subpopulation shift. In *International Conference on Machine Learning*, pages 39584–39622. PMLR, 2023. [5](#)
- [65] Jiahui Yu, Xin Li, Jing Yu Koh, Han Zhang, Ruoming Pang, James Qin, Alexander Ku, Yuanzhong Xu, Jason Baldridge, and Yonghui Wu. Vector-quantized image modeling with improved vqgan. *arXiv preprint arXiv:2110.04627*, 2021. [3](#)
- [66] Jiahui Yu, Yuanzhong Xu, Jing Yu Koh, Thang Luong, Gunjan Baid, Zirui Wang, Vijay Vasudevan, Alexander Ku, Yinfei Yang, Burcu Karagol Ayan, et al. Scaling autoregressive models for content-rich text-to-image generation. *arXiv preprint arXiv:2206.10789*, 2(3):5, 2022. [3](#)

A. Further Details

A.1. Datasets for Group Robustness

Here, we detail the task of each dataset for group robustness. In Table 4, we also tabulate the labels and attributes that define each subgroup along with their sample sizes.

Waterbirds. Given an image of a bird, the task is to predict whether it is a waterbird or landbird [57]. The attribute is the background that the bird is on [47].

CelebA. Given an image of a person, the task is to predict whether their hair color is blond or not [33]. The attribute is the binary gender of the person.

MetaShift. Given an image of an animal, the task is to predict whether it is a dog or cat [29]. The attribute is the environment that the dog or cat is in.

Dataset	Subgroup	Label	Attribute	Training	Validation	Test
Waterbirds	0	0 (landbird)	0 (on land)	3498	467	2255
	1	0 (landbird)	1 (on water)	184	466	2255
	2	1 (waterbird)	0 (on land)	56	133	642
	3	1 (waterbird)	1 (on water)	1057	133	642
CelebA	0	0 (non-blond)	0 (woman)	71629	8535	9767
	1	0 (non-blond)	1 (man)	66874	8276	7535
	2	1 (blond)	0 (woman)	22880	2874	2480
	3	1 (blond)	1 (man)	1387	182	180
MetaShift	0	0 (dog)	0 (outdoor)	784	127	273
	1	0 (dog)	1 (indoor)	507	75	191
	2	1 (cat)	0 (outdoor)	196	33	65
	3	1 (cat)	1 (indoor)	789	114	345

Table 4. Defined subgroups in Waterbirds, CelebA, and MetaShift.

B. Supplementary Experiments

Here, we detail the supplementary experiments that we conducted. First, we explore additional design choices and effects of the inter-image approach. Appendix B.1 shows the ineffectiveness of patch matching with visual words formed in the embedding space. In Appendix B.2, random matching is applied to further determine if matching by the visual words are meaningful. Appendix B.3 ablates the similarity threshold by relaxing it for further compression. The fairness of tokenization and sparsity of the vocabulary are shown in Appendices B.4 and B.5, respectively.

B.1. Ineffectiveness of the Embedding Space

In Table 5, we analyze the sequence compression using visual words formed in the embedding space. To do so, we initialize each vocabulary by clustering embeddings from the pre-trained convolution layer of CLIP or BLIP. During inference, we match the activations from the pre-trained convolution layer with the visual words. Compared to Table 1, we observe a notable reduction in the degree of compression irrespective of pre-processing data and vocabulary size. In [50], embeddings are shown to become progressively more similar to one another due to self-attention. Hence, it is unsurprising that matching activations and visual words at the beginning of the network is ineffective.

B.2. Random Matching of Visual Words

In Table 6, we study the effects of randomly matching the patches. We initialize the pairwise cosine distance by sampling from a uniform distribution of $[0, 2]$. First, we find the token length (including [CLS]) to differ noticeably from Table 1. For $\mathcal{T}_{inter}^{100}$, sequences are further reduced across the datasets. Conversely, $\mathcal{T}_{inter}^{1000}$ and $\mathcal{T}_{inter}^{10000}$ display little compression. Second, performance is shown to change from Table 3. We observe a significant degradation in average and worst-group accuracies

with $\mathcal{T}_{inter}^{100}$ on Waterbirds and MetaShift. For $\mathcal{T}_{inter}^{1000}$ and $\mathcal{T}_{inter}^{10000}$, performance does not shift much from *Base* as barely any compression occurs. With random matching, the captions become completely different than those of *Base* in Figure 10.

B.3. Ablation of the Similarity Threshold

We have shown how VWTs can improve the efficiency of online inference. To better understand their limitations, we ablate the threshold of $\mathcal{T}_{inter}^{100}$ by setting it to values of $\{0.2, 0.3, 0.4, 0.5\}$ in Table 7. We seek to determine if exploiting higher thresholds for increased compression is a viable strategy. Naturally, we observe a reduction in performance as increasingly dissimilar patches are merged. For Waterbirds and MetaShift, the worst-group accuracy degrades more significantly than the average, especially with the former. Interestingly, average accuracy remains relatively unchanged while worst-group accuracy improves significantly on CelebA irrespective of similarity threshold. We posit that at higher thresholds, the merging of core features represented by the foreground object results in the reduced performance of Waterbirds and MetaShift.

B.4. Fairness of the Tokenization

On text data, tokenizers have been shown to induce unfairness between languages [2, 41]. Since most LLMs are built using English data, tokenization of minority languages produces inherently longer sequences that raises compute costs. We seek to analyze if similar effects exist with VWTs as well. In Table 8, we show the breakdown in token length (including [CLS]) and accuracy (w.r.t *Base*) by subgroup. First, we observe a notable difference in compression between the subgroups of Waterbirds. With \mathcal{T}_{100} , sequences might differ by up to 39 tokens as seen with subgroups 0 and 3. Smaller discrepancies are displayed on CelebA and MetaShift except for \mathcal{T}_{100} on the former. Second, we find that compression does not affect all subgroups equally. Accuracy improves on certain subgroups and degrades on others. A stronger compression does not correlate also with a large change in performance. Like text tokenizers, VWTs may induce inequality in compression that leads to varying inference costs and performance for different subgroups.

B.5. Sparsity of the Vocabulary

To better understand the utilization of the visual words, we plot the probability distribution of the matches in Figure 6. Regardless of the dataset, we find that certain visual words are matched more frequently than others, thus leading to a large skew in the distributions. Greater sparsity is also displayed by larger vocabularies as many visual words remain unused across datasets. As such, pruning may be applied to achieve a more efficient vocabulary size post-clustering.

C. Additional Results

Here, we provide additional results by other models and hyperparameters in our experiments. Appendix C.1 lists long-form captions by Q_8 , *ToME*, and $\mathcal{T}_{inter}^{10000}$. Appendices C.2 and C.3 detail the intra-image and inter-image approaches with various dropping ratios and vocabulary sizes, respectively.

C.1. Long-form Captions

In Figure 7, we showcase long-form captions by Q_8 , *ToME*, and $\mathcal{T}_{inter}^{10000}$. First, we observe improvements in the accuracy of the descriptions with Q_8 over *Base* in Figure 4. Although the captions relate better to the image, the overall length is shorter than those of other methods. The generation may continue to introduce unnecessary repetitions. Second, we find *ToME* and $\mathcal{T}_{inter}^{10000}$ to also be beneficial for descriptiveness and coherence. On certain samples, repeating n-grams may still occur.

C.2. Dropping Ratio

Following [39], we apply the intra-image approach with ratios of $\{0.25, 0.33, 0.7\}$ to the total number of patches in Table 9. We observe a natural degradation as the ratio increases with performance dropping steeply at 0.7. In Figures 8 and 9, we visualize the dropped patches and captions on COCO, respectively. In most cases, the patches with the lowest pixel variance correspond to uninformative backgrounds. Dropping such patches may continue to preserve the foreground object.

C.3. Vocabulary Size

In Table 10, we apply the inter-image approach with vocabulary sizes of $\{100, 10000\}$. We find performance to be noticeably lower than *Base* in Table 3 with the smaller vocabulary of $\mathcal{T}_{inter}^{100}$. Meanwhile, performance retention is higher for $\mathcal{T}_{inter}^{10000}$ due to lower sequence compression in Table 1. When visualizing the captions on COCO in Figure 10, we also observe that increasing thresholds cause larger deviations from *Base* than reducing the vocabulary size.

Dataset	$\mathcal{T}_{inter}^{100}$		$\mathcal{T}_{inter}^{1000}$		$\mathcal{T}_{inter}^{10000}$	
	In-Domain	ImageNet	In-Domain	ImageNet	In-Domain	ImageNet
Waterbirds	180	179	179	179	182	182
CelebA	153	154	157	154	170	165
MetaShift	176	173	175	174	180	180
COCO	405	406	409	408	442	440
NoCaps	-	394	-	396	-	431

Table 5. Token length per sample (including [CLS]). Tokenizers of varying pre-processing data and vocabulary sizes are shown. Visual words are formed from **embeddings** in the pre-trained convolution layer of CLIP or BLIP and not the image patches. Poor compression is seen irrespective of pre-processing data and vocabulary size due to the lack of similarity between the activations and visual words.

Dataset	Model	$\mathcal{T}_{intra}^{100}$	$\mathcal{T}_{intra}^{1000}$	$\mathcal{T}_{intra}^{10000}$
Waterbirds	CLIP	88	179	195
CelebA				
MetaShift				
OpenImages (Com.)				
OpenImages (Rare)				
COCO	BLIP	104	439	561
NoCaps				

(a) Length

Model	Waterbirds		CelebA		MetaShift		Overall \uparrow	
	Average \uparrow	Worst \uparrow	Average \uparrow	Worst \uparrow	Average \uparrow	Worst \uparrow	Common \uparrow	Rare \uparrow
$\mathcal{T}_{inter}^{100}$	66.60 \pm 0.28	9.61 \pm 1.51	90.24 \pm 0.06	56.48 \pm 4.32	76.16 \pm 0.70	61.43 \pm 1.32	41.06	39.84
$\mathcal{T}_{inter}^{1000}$	78.10 \pm 0.18	22.74 \pm 1.24	90.25 \pm 0.15	47.96 \pm 2.24	94.20 \pm 0.63	87.18 \pm 1.78	70.29	63.48
$\mathcal{T}_{inter}^{10000}$	78.98 \pm 0.07	21.96 \pm 0.31	89.61 \pm 0.07	47.46 \pm 2.62	95.27 \pm 0.97	87.18 \pm 2.35	70.52	63.40

(b) CLIP (image classification and group robustness)

Model	COCO		NoCaps							
	Karpathy \uparrow		In-Domain \uparrow		Near-Domain \uparrow		Out-of-Domain \uparrow		Overall \uparrow	
	BLEU@4	CIDEr	CIDEr	SPICE	CIDEr	SPICE	CIDEr	SPICE	CIDEr	SPICE
$\mathcal{T}_{inter}^{100}$	9.92	19.18	15.81	7.20	10.95	6.25	10.55	6.63	11.57	6.47
$\mathcal{T}_{inter}^{1000}$	32.06	100.52	96.87	14.04	91.83	13.47	89.52	12.96	92.09	13.45
$\mathcal{T}_{inter}^{10000}$	34.04	107.35	103.55	14.49	98.22	14.00	94.08	13.48	98.15	13.97

(c) BLIP (image captioning)

Table 6. Token length (including [CLS]) and performance of VWTs with random matching. The pairwise cosine distance is initialized by sampling from a uniform distribution of $[0, 2]$. Average and worst-group accuracies degrade noticeably with \mathcal{T}_{100} except for CelebA. Performance does not change much for \mathcal{T}_{1000} and \mathcal{T}_{10000} from *Base* since barely any compression occurs.

Dataset	Thresh	Length	Average \uparrow	Worst \uparrow
Waterbirds	0.2	97	76.71 ± 0.24	24.09 ± 0.59
	0.3	79	74.85 ± 0.15	21.13 ± 0.36
	0.4	66	73.35 ± 0.12	16.30 ± 0.24
	0.5	58	72.81 ± 0.10	13.14 ± 0.48
CelebA	0.2	66	89.44 ± 0.08	56.48 ± 1.70
	0.3	55	88.85 ± 0.26	58.70 ± 4.21
	0.4	50	88.31 ± 0.14	57.04 ± 3.26
	0.5	48	88.21 ± 0.32	55.74 ± 1.40
MetaShift	0.2	84	86.16 ± 0.89	77.46 ± 2.34
	0.3	69	81.16 ± 1.00	67.77 ± 1.43
	0.4	60	77.73 ± 1.03	60.65 ± 2.57
	0.5	55	74.75 ± 1.36	56.08 ± 3.38

Table 7. Token length (including [CLS]) and performance using $\mathcal{T}_{inter}^{100}$ with varying similarity thresholds. Higher thresholds can reduce sequences to 48 tokens on CelebA. Greater compression results in higher degradation in performance, particularly in robustness.

Model	Subgroup	Waterbirds		CelebA		MetaShift	
		Length	Δ Accuracy	Length	Δ Accuracy	Length	Δ Accuracy
<i>Base</i>	0		98.89		95.63		98.54
	1	197	82.45	197	96.23	197	93.19
	2		21.86		48.67		87.69
	3		54.73		50.00		95.36
$\mathcal{T}_{inter}^{100}$	0		144		-0.67		85
	1	106	-3.82	88	-0.13	110	-6.18
	2	140	19.00	98	32.62	119	-2.92
	3	105	6.17	99	6.30	100	-9.02
$\mathcal{T}_{inter}^{1000}$	0	160	-0.40	119	-0.46	138	-0.25
	1	129	-0.22	117	0.74	138	-2.06
	2	160	9.03	124	18.92	143	-1.17
	3	129	2.18	124	-4.07	131	-2.13
$\mathcal{T}_{inter}^{10000}$	0	180	-0.09	158	0.25	163	-0.37
	1	156	1.34	151	0.66	167	0.19
	2	181	4.75	158	2.96	169	-1.75
	3	158	1.71	156	-6.30	163	-0.81

Table 8. Distribution of token length (including [CLS]) and accuracy (w.r.t. *Base*) by subgroup. Tokenizers of varying vocabulary sizes are shown. Like text tokenizers, VWTs may induce significantly unequal token lengths as seen with $\mathcal{T}_{inter}^{100}$ on Waterbirds. Subgroups are also affected unequally as stronger compression does not correlate with greater improvement or degradation in performance.

Dataset	Model	$\mathcal{T}_{intra}^{0.25}$	$\mathcal{T}_{intra}^{0.33}$	$\mathcal{T}_{intra}^{0.7}$
Waterbirds CelebA MetaShift OpenImages (Com.) OpenImages (Rare)	CLIP	148	132	59
COCO NoCaps	BLIP	433	386	173

(a) Length

Model	Waterbirds		CelebA		MetaShift		OpenImages	
	Average \uparrow	Worst \uparrow	Average \uparrow	Worst \uparrow	Average \uparrow	Worst \uparrow	Common \uparrow	Rare \uparrow
$\mathcal{T}_{intra}^{0.25}$	78.31 \pm 0.09	26.69 \pm 0.24	89.46 \pm 0.16	48.47 \pm 1.56	94.70 \pm 0.43	87.69 \pm 1.54	69.79	63.37
$\mathcal{T}_{intra}^{0.33}$	77.72 \pm 0.24	27.78 \pm 0.48	89.31 \pm 0.22	48.83 \pm 1.42	94.62 \pm 0.41	87.18 \pm 2.35	69.11	62.75
$\mathcal{T}_{intra}^{0.7}$	73.27 \pm 0.12	18.80 \pm 0.32	89.19 \pm 0.05	45.37 \pm 1.28	82.61 \pm 1.10	63.59 \pm 0.89	46.83	42.68

(b) CLIP (image classification and group robustness)

Model	COCO		NoCaps							
	Karpthy \uparrow		In-Domain \uparrow		Near-Domain \uparrow		Out-of-Domain \uparrow		Overall \uparrow	
	BLEU@4	CIDEr	CIDEr	SPICE	CIDEr	SPICE	CIDEr	SPICE	CIDEr	SPICE
$\mathcal{T}_{intra}^{0.25}$	33.92	107.47	103.59	14.65	98.39	14.07	94.47	13.59	98.34	14.06
$\mathcal{T}_{intra}^{0.33}$	33.59	106.25	103.19	14.65	97.40	13.95	92.66	13.41	97.27	13.95
$\mathcal{T}_{intra}^{0.7}$	29.64	93.20	89.89	13.53	85.04	12.82	80.81	12.31	84.88	12.82

(c) BLIP (image captioning)

Table 9. Token length (including [CLS]) and performance of VWTs with varying dropping ratios.

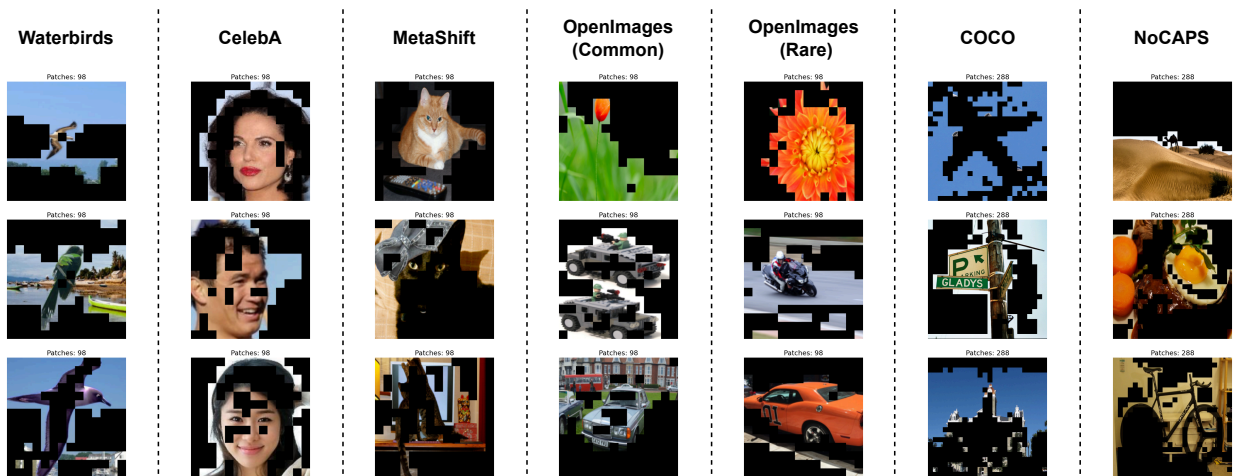
Figure 8. Visualization of patch dropping by our visual word tokenizer ($\mathcal{T}_{intra}^{0.5}$ model). Patches with the lowest pixel variance that are dropped are indicated in black. In most cases, the dropped patches correspond to the background object that is typically uninformative.



Figure 9. Visualization of captions by token dropping on COCO. Token dropping of up to 0.5 may not cause significant deviation in the generations from the base model. On certain samples, the accuracy of the descriptions can improve as well.

Model	Waterbirds		CelebA		MetaShift		OpenImages	
	Average \uparrow	Worst \uparrow	Average \uparrow	Worst \uparrow	Average \uparrow	Worst \uparrow	Common \uparrow	Rare \uparrow
$\mathcal{T}_{inter}^{100}$	78.41 \pm 0.09	26.01 \pm 0.41	90.04 \pm 0.22	53.15 \pm 3.21	90.24 \pm 0.40	84.28 \pm 2.38	62.90	58.10
$\mathcal{T}_{inter}^{10000}$	79.68 \pm 0.11	22.90 \pm 0.16	90.12 \pm 0.18	46.85 \pm 4.63	94.81 \pm 0.95	86.15 \pm 1.54	69.03	62.50

(a) CLIP (image classification and group robustness)

Model	COCO		NoCaps							
	Karpathy \uparrow		In-Domain \uparrow		Near-Domain \uparrow		Out-of-Domain \uparrow		Overall \uparrow	
	BLEU@4	CIDEr	CIDEr	SPICE	CIDEr	SPICE	CIDEr	SPICE	CIDEr	SPICE
$\mathcal{T}_{inter}^{100}$	31.10	97.70	95.58	13.78	89.62	13.11	82.42	12.44	89.02	13.08
$\mathcal{T}_{inter}^{10000}$	33.18	105.08	102.84	14.59	98.03	13.95	91.52	13.14	97.40	13.88

(b) BLIP (image captioning)

Table 10. Token length (including [CLS]) and performance of VWTs with varying vocabulary sizes.



Figure 10. Visualization of captions by VWTs on COCO. Increasing the similarity threshold causes the generated captions to deviate more than reducing the vocabulary size. With random matching, the model begins to completely misunderstand the image.